

Diamond Sensors in HEP

CERN RD-42 Collaboration

M.Mikuž^{1,12}, M.Artuso²⁴, F.Bachmair²⁸, L.Bäni²⁸, V.Bellini², V.Belyaev¹⁵, E.Berdermann⁸, J-M.Brom¹⁰, M.Bruzzo⁵, B. Caylar¹⁴, M.Červ³, G.Chiodini³¹, D.Chren²², V.Cindro¹², G.Claus¹⁰, M.Cristinziani¹, S.Costa², J.Cumalat²³, R.D'Alessandro⁶, W.de Boer¹³, D.Dobos³, W.Dulinski¹⁰, V.Eremin⁹, R.Eusebi²⁹, H.Frais-Kölbl⁴, C.Gallrapp³, K.K.Gan¹⁶, J.Garofoli²⁴, M.Gastal³, M.Goffe¹⁰, J.Goldstein²⁰, A.Golubev¹¹, L.Gonella¹, A.Gorišek¹², E.Grigoriev¹¹, J.Grosse-Knetter²⁷, M.Guthoff¹³, I.Haughton²⁶, D.Hidas¹⁷, D.Hits²⁸, M.Hoeferkamp²⁵, J.Hosselt¹⁰, F.Hüggling¹, H.Jansen³, J.Janssen¹, H.Kagan¹⁶, R.Kass¹⁶, G.Kramberger¹², S.Kuleshov¹¹, S.Kwan⁷, S.Lagomarsino⁶, A.Lo Giudice¹⁸, C.Maazouzi¹⁰, I.Mandić¹², C.Manfredotti¹⁸, C.Manfredotti¹⁸, A.Martemyanov¹¹, C.Mathieu¹⁰, H.Merritt¹⁶, M.Moench²⁸, R.Mori⁵, J.Moss¹⁶, R.Mountain²⁴, G.Oakham²¹, T.Obermann¹, A.Oh²⁶, P.Olivero¹⁸, G.Parrini⁶, H.Pernegger³, R.Perrino³¹, M.Pomorski¹⁴, R.Potenza², A.Quadt²⁷, S.Roe³, S.Schnetzler¹⁷, T.Schreiner⁴, S.Saidel²⁵, A.Sfyrla³, S.Sciortino⁶, S.Smith¹⁶, B.Sopko²², S.Spagnolo³¹, S.Spanier³⁰, K.Stenson²³, R.Stone¹⁷, C.Sutera², W.Trischuk¹⁹, C.Tuve², V.Tyzhnevyyi²⁶, L.Upleger⁷, J.Velthuis²¹, N.Venturi¹⁹, E.Vittone¹⁸, S.Wagner²³, R.Wallny²⁸, J.C.Wang²⁴, R.Wang²⁵, P.Weilhammer³, J.Weingarten²⁷, C.Weiss³, T.Wengler³, N.Wermes¹, M.Zavrtanik¹²

¹Universität Bonn, Bonn, Germany, ²INFN/University of Catania, Catania, Italy, ³CERN, Geneva, Switzerland, ⁴Fachhochschule für Wirtschaft und Technik, Wiener Neustadt, Austria, ⁵INFN/University of Florence, Florence, Italy, ⁶Department of Energetics/INFN, Florence, Italy, ⁷FNAL, Batavia, USA, ⁹Ioffe Institute, St. Petersburg, Russia, ¹⁰IPHC, Strasbourg, France, ¹¹ITEP, Moscow, Russia, ¹²Jožef Stefan Institute and Physics Department, University of Ljubljana, Ljubljana, Slovenia, ¹³Universität Karlsruhe, Karlsruhe, Germany, ¹⁴CEA/LIST Technologies Avancées, Saclay, France ¹⁵MEPHI Institute, Moscow, Russia, ¹⁶The Ohio State University, Columbus, OH, USA, ¹⁷Rutgers University, Piscataway, NJ, USA, ¹⁸University of Torino, Torino, Italy, ¹⁹University of Toronto, Toronto, Canada, ²⁰University of Bristol, Bristol, UK, ²¹Carleton University, Ottawa, Canada, ²²Czech Technical University, Prague, Czech Republic, ²³University of Colorado, Boulder, CO, USA, ²⁴Syracuse University, Syracuse, NY, USA, ²⁵University of New Mexico, Albuquerque, NM, USA, ²⁶University of Manchester, Manchester, UK, ²⁷Universität Göttingen, Göttingen, Germany, ²⁸ETH Zürich, Zürich, Switzerland, ²⁹Texas A&M College, Park Station, TX, USA, ³⁰University of Tennessee, Knoxville, TN, USA, ³¹INFN-Lecce, Lecce, Italy.

¹Speaker, E-mail: Marko.Mikuz@ijs.si

ABSTRACT

With the first three years of the LHC running well underway, and luminosity upgrades expected towards the end of the decade, ATLAS and CMS are planning to upgrade their innermost tracking layers with the utmost radiation hard technologies. Chemical Vapour Deposition (CVD) diamond has been used extensively in beam conditions monitors as the innermost detectors in the highest radiation areas of BaBar, Belle, CDF and all LHC experiments. This material is now being considered as a sensor material for the innermost layer(s) of the upgraded trackers. Recently the CERN RD42 collaboration constructed, irradiated and tested polycrystalline and single-crystal CVD diamond sensors to the highest fluences expected at the innermost tracking layers of the HL-LHC. We present beam test results of chemical vapour deposition diamond to fluences in excess of 10^{16} protons/cm² illustrating that both polycrystalline and single-crystal chemical vapour deposition diamonds follow a single damage curve. We briefly describe the performance of the diamond-based ATLAS beam monitoring devices and discuss plans for their upgrade to a diamond tracker during the 2013/14 LHC consolidation shut-down.

*36th International Conference on High Energy Physics
July 4-11, 2012
Melbourne, Australia*

1. Introduction

Progress in experimental particle physics in the coming decade depends crucially upon the ability to carry out experiments at high energies and high luminosities. These conditions imply that future experiments will take place in extremely harsh radiation areas, with hadron fluences surpassing $10^{16}/\text{cm}^2$ for innermost tracking layers or even 10^{17} in forward calorimeters. In order to perform these complex and expensive experiments new radiation hard technologies are being developed. Chemical Vapour Deposition (CVD) diamond is being pursued by the CERN RD-42 collaboration [1] as a radiation tolerant material for use very close to the interaction region. During the past few years many CVD diamond devices have been manufactured and tested. As a detector for high radiation environments CVD diamond benefits substantially from its intrinsic radiation hardness (large displacement energy 42 eV/atom), very low leakage current, low dielectric constant, fast signal collection and ability to operate at room temperature. As a result CVD diamond now has been used extensively in beam conditions monitors as the innermost detectors in the highest radiation areas of colliders. CVD diamond is being considered as a sensor material for the future particle tracking detectors closest to the interaction region where the most extreme radiation conditions exist. We present the state-of-the-art of the radiation tolerance of the highest quality CVD diamond material for a range of proton energies, pions and neutrons obtained from strip detectors constructed with this material.

Recently single crystal CVD diamond material has been developed which resolves many of the issues associated with polycrystalline material. We also present recent results on radiation tolerance obtained from strip detectors constructed from this new diamond material. We discuss the use of diamond detectors and their survivability in the highest radiation environments.

Currently diamond is deployed in HEP experiments for two tasks: for beam conditions monitoring and measurement of luminosity. Beam conditions can be deduced either from beam induced current measurements replacing the commonly used ionization chambers by CVD diamond pad detectors (e.g. ATLAS BLM; CMS BCM1, BCM2, LHCb, ALICE) or by particle counting (ATLAS BCM; CMS BCMF). Due to its fast response and insensitivity to pile-up, ATLAS BCM also serves as the preferred luminosity monitor. As a result of positive experience with the ATLAS BCM an upgraded Diamond Beam Monitor (DBM) is being prepared for installation during the 2013-14 LHC shutdown. This detector will be a true diamond sensor based tracker, consisting of 8 three-layer telescopes of pixelated diamond detectors. Each plane will have $\sim 27\text{k}$ active pixels. The telescopes will provide sub-mm impact parameter resolution adding spatial information on the origin of backgrounds to the already precise (sub-ns) timing information from the BCM.

2. Diamonds as Particle Detectors

Diamond, because of its large resistivity, can be operated as a solid-state ionization chamber. In Fig. 1, the basic principle of using diamond as a particle detector is shown [2]. A voltage is applied across a layer of diamond a few hundred microns thick. When a charged particle traverses the diamond, atoms in crystal lattice sites are ionized, promoting electrons into the conduction band and leaving holes in the valence band. On average, 36 electron-hole pairs

are created in each μm of diamond traversed by a minimum ionizing particle. These charges drift across the diamond in response to the applied electric field producing a detectable electric signal. Since there may be traps in CVD material we often use the charge collection distance (*CCD*) to characterize the material. *CCD* corresponds to the average distance the electron-hole pairs move apart. In thin diamond *CCD* is limited by sensor dimension, while in thick (thickness $\gg \text{CCD}$) diamond *CCD* approaches the sum of mean free paths of electrons and holes.

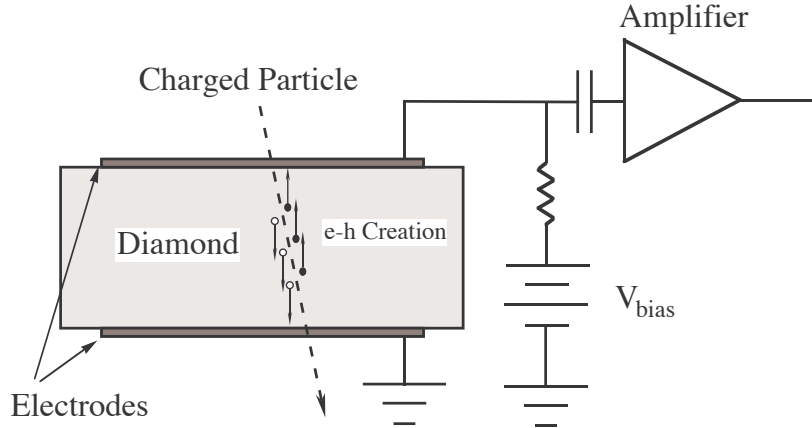


Figure 1: Schematic view of operation of a diamond particle detector. The metal electrodes can be segmented to produce a pixel or strip detector.

There are two flavours of CVD diamond: polycrystalline (pCVD) and single crystal (scCVD). The scCVD is grown on a high-pressure high-temperature diamond substrate and forms a perfect diamond lattice. On the other hand, pCVD is grown on a non-diamond substrate, therefore small crystal grains in random orientations start forming on the substrate. The grains grow, and the larger ones have the tendency to grow faster, terminating the growth of the smaller ones. Therefore the average grain size increases across the pCVD thickness from the substrate to the growth side. Also the charge collection properties of the material exhibit improvement with growth thickness.

While scCVD exhibits very little trapping, and therefore its *CCD* matches the detector thickness, *CCD* of pCVD's is limited by trapping. It is helpful to grow thick pCVD wafers, with thickness in excess of 1 mm, and polish off the substrate side, keeping the high quality material with large grains. Top quality pCVD material today can be grown in 6" wafers, and can exhibit *CCD* close to 300 μm at 500 μm thickness and electric field of 2 V/ μm . The superb quality of scCVD is for the time heavily offset by size and price; scCVD, in contrast to 6" pCVD wafers, is limited to sizes of 1x1 cm^2 , and the price difference for the small pieces available is nearly an order of magnitude.

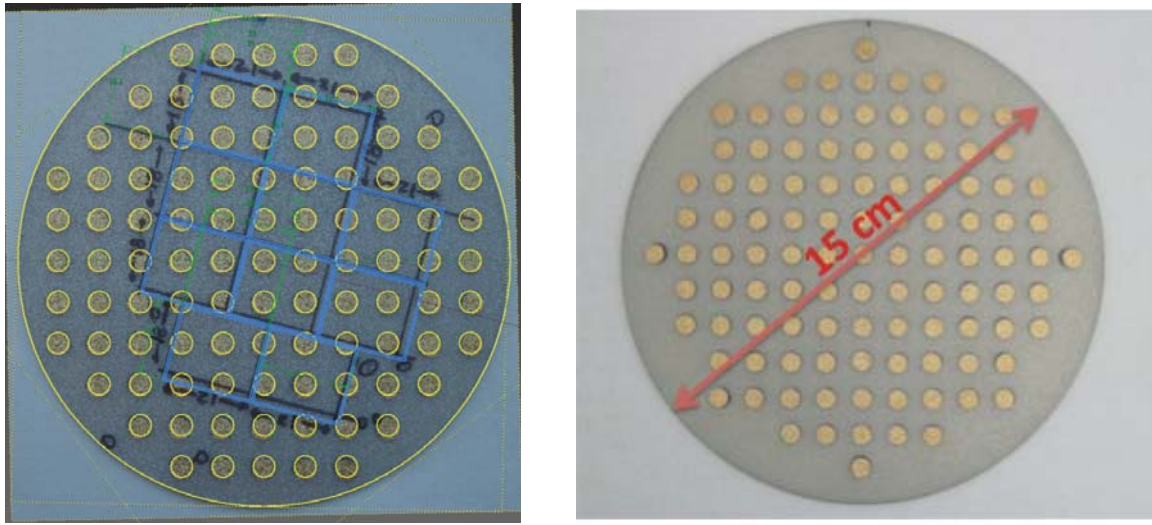
3. Diamond Sensor Suppliers

Traditionally all supplies of electronic grade diamond for HEP applications came from a single manufacturer [3] despite all efforts of CERN RD-42 to establish additional suppliers and foster competition, especially in view of a potentially sizeable demand of sensors for a HL-LHC tracking layer. Established with the aim of marketing electronic grade diamond the producer ran

into commercial difficulties to the point in May 2012 when the owners decided not to sustain operation. Partly its mission is maintained by one of the former owners who are offering the same product line under their own brand name [4]. In 2012 a newly grown 5" pCVD wafer was obtained for testing (Fig.2a). Ten regions of $\sim 2\text{ cm} \times 2\text{ cm}$ were selected on this wafer and the 10 diamond sensors were delivered as part of the ATLAS Diamond Beam Monitor (DBM) project.

Following successful trial results, an additional manufacturer [5], regularly producing optical grade diamond, offered sensors for the ATLAS DBM. A wafer of 6" size was grown to honour an order of ten $2\text{ cm} \times 2\text{ cm}$ sensors (Fig. 2b).

Figure 2: Recent pCVD diamond wafers delivered: 2a(left): Wafer from [4], 5" diameter, with test-dots on a 1 cm grid. Markings delimit cut-outs for ten DBM sensors. 2b(right): 6" wafer from [5] with the equivalent test-dot pattern.



4. Radiation Damage

Diamond, because of its intrinsically large displacement energy of 42 eV per atom (26 eV for Si), is believed to exhibit favourable radiation resistance. In contrast to silicon, radiation-induced levels exhibit no noticeable effect on the leakage current, as even if located close to mid-gap ($E_t \sim 2.5\text{ eV}$) they can't act as generation centres at room temperature. They can, however, as in radiation-damaged silicon, trap drifting charge. If sufficiently separated from the conduction band (*deep traps*) the de-trapping times are large, even of order of months, so the charge is lost for the signal. Usually an occupied trap cannot trap the same charge carrier, so it remains passivized for the de-trapping time. It can, however, trap the carrier of the opposite charge, effectively serving as a recombination centre. The cross sections for the capture of the two carrier species (electrons and holes) can differ by orders of magnitude, with the larger cross section exhibited by a charged (empty) trap than the neutral (filled) one. This forms the fundament of the "pumping" procedure, where diamonds are exposed to ionizing radiation, which fills the traps and passivizes them. Pumping is done before the measurement using a strong ^{90}Sr source. It is inherently present in hadron colliders where tracking detectors are exposed to charged particle fluxes in excess of MHz/cm^2 .

Pumping could in principle affect the space charge and thus the electric field distribution in the sensor bulk. As no strong effects are observed one could conclude that the trapping of electrons and holes is of similar probability, thus the resulting space charge largely cancels out.

Traps can be present already in non-irradiated diamond because of lattice imperfections or be radiation-induced as a result of atom displacements. The former should be more abundant in the less perfect pCVD diamond, where in addition charge can also be trapped on grain boundaries. The introduction traps by radiation can be thought as non-discriminating between the two CVD diamond flavours, pCVD and scCVD, and the two trapping sources should be additive. As the mean free path (mfp) of each carrier is inversely proportional to the relevant trap density, the resulting model is written as:

$$\frac{1}{mfp_{e,h}} = \frac{1}{mfp_{0,e,h}} + k_{mfp,e,h} \times \Phi, \quad (1)$$

with k_{mfp} the radiation damage constant and mfp_0 the value of mfp before irradiation.

In thick detectors CCD , being equal to the sum of $mfp_{e,h}$, is observed to follow the sum of two hyperbolae given by Eq. (1), which add up to a single hyperbola with $1/mfp_0 = 1/mfp_{0,e} + 1/mfp_{0,h}$ and $k_{mfp} = k_{mfp,e} + k_{mfp,h}$. Empirically, measuring CCD with strip detectors, the collected signal is quasi independent on the electric field direction, indicating that mfp of electrons roughly matches that of the holes ($mfp_e \sim mfp_h$).

For thinner detectors the detector dimension limits the measured CCD . As the extreme case, non-irradiated scCVD exhibits an essentially infinite mfp_0 , thus there CCD equals the detector thickness. For intermediate thicknesses the correspondence between CCD and $mfp = mfp_e + mfp_h$ in the assumption $mfp_e \sim mfp_h$ is given by:

$$CCD = 2 \times mfp \left[1 - \frac{mfp}{t} (1 - \exp(-\frac{t}{mfp})) \right], \quad (2)$$

where t is the detector thickness.

Ideally, to test for radiation hardness, detectors should be irradiated with the particle spectrum encountered at the targeted application. For LHC and its upgrades the prevalent species close to the interaction region are pions, their spectrum peaked at ~ 2 GeV, with FWHM from 300 MeV to 6 GeV [6]. Such irradiation facilities do not exist, at least not in the sought fluence range. Therefore damage modelling is needed. Often the damage is taken proportional to non-ionizing energy loss (NIEL) of the respective particle. The NIEL assumption proved useful for silicon, although also there departures from predictions have been observed. With the sources available, it sounds plausible to concentrate on charged hadrons of similar energy, and then do the residual scaling with interpolation. Luckily enough, the CERN PS irradiation facility with 24 GeV protons and the LANL LANSCE facility with 800 MeV protons bridge the relevant energy region. Models predict damage variation of factor 2 (NIEL based – [7]) or even only 20 % (displacement per atom (DPA) based – [8]) across this energy interval.

Four diamond sensors have been irradiated at each facility, 2 pCVD and 2 scCVD at CERN, and 3 pCVD and 1 scCVD at Los Alamos. The administrated fluence spans the range relevant for the HL-LHC upgrade. CCD was obtained before irradiation and after each irradiation step by turning the sensor into a strip detector and measuring its response to the CERN SPS high-energy pion test beam. For each of the sensors, fluence dependence was fitted

with the linearized form of Eq. 1 ($1/mfp$ vs. fluence – Figs. 3). Eq. 2 was used to obtain mfp from the measured CCD , with mfp_0 either deduced from measured CCD before irradiation or taken as infinite for the scCVD samples. Errors on CCD and fluence were obtained from the measurement or given by the irradiation facilities, respectively, and are typically about 10 % of the respective values. A linear fit with k_{mfp} and mfp_0 as the free parameters was performed, where the fitted mfp_0 is relevant only for samples with more than one irradiation step.

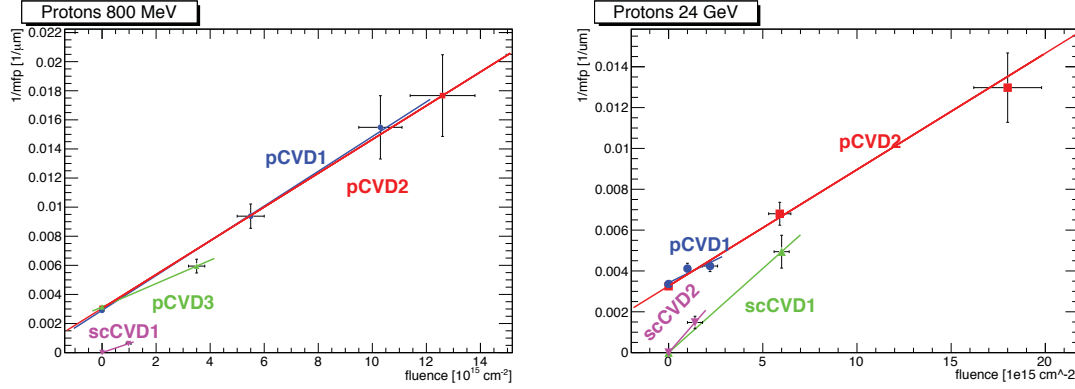


Figure 3: Dependence of $1/mfp$ vs. fluence for irradiations with 800 MeV protons at LANL (left) and 24 GeV protons at CERN. Each of the four diamonds is fitted with a linear model according to Eq. 2.

The resulting k_{mfp} for all the samples are depicted in Figs. 4. They appear consistent among each other, indicating a common mechanism of radiation damage. The consistency in averaging the samples is manifested better on the 24 GeV data, although also the average χ^2 for the 800 MeV data amounts to an acceptable 7.3 for 3 degrees of freedom. The resulting average k_{mfp} are $(0.62 \pm 0.07) \times 10^{-18} \mu m^{-1} cm^{-2}$ for 24 GeV and $(0.95 \pm 0.09) \times 10^{-18} \mu m^{-1} cm^{-2}$ for 800 MeV protons. The damage ratio seems to favour the DPA prediction, but one should treat these results as preliminary: data and their errors are still being scrutinized, and there is more data to be added to the analysis.

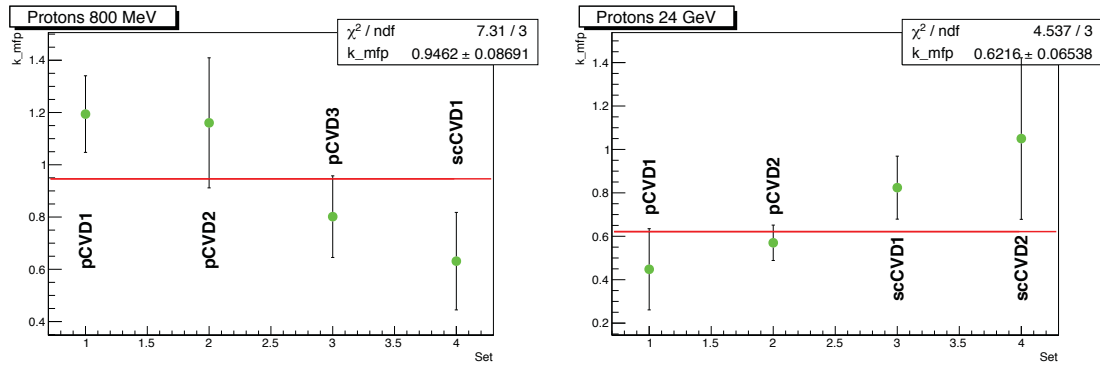


Figure 4: Consistency of the four k_{mfp} at each proton energy obtained from the fit in Fig. 3: 800 MeV protons (left) and 24 GeV protons (right). The line denotes a constant fit to the four values, the fit result and χ^2 indicated in the figures

Having obtained average k_{mfp} for each data set it is possible to exhibit consistency of various samples with Eq. 1 by using k_{mfp} to turn mfp_0 into a fluence offset $\Phi_0 = (k_{mfp} \cdot mfp_0)^{-1}$. This

offset is of order of $3\text{-}5 \times 10^{15} \text{ cm}^{-2}$ for pCVD of today's state-of-the-art quality, and can be regarded as the fluence headroom if one were able to use ultimate quality (scCVD) diamond instead. The resulting plots are shown in Figs. 5 with one-sigma bands indicated. All results conform to Eq. 1 to better than 2 sigma, demonstrating validity of the assumption of a common radiation damage mechanism in CVD diamond.

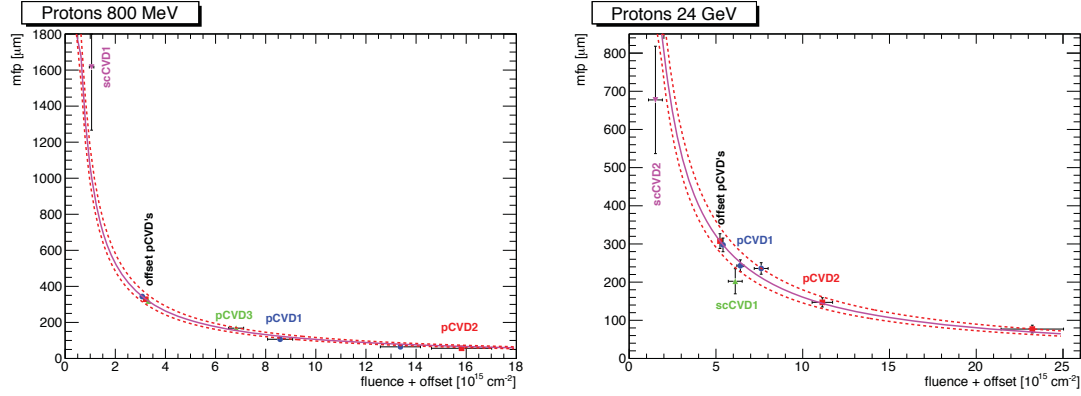


Figure 5: Plot of all irradiation data: 800 MeV protons (left) and 24 GeV protons (right). The line denotes Eq. 2 with the average k_{mfp} and infinite initial mfp . The pCVD diamond points have been offset as discussed in the text. The dotted line represents variation of k_{mfp} by one standard deviation.

Neutrons constitute a minor part of order of 10 % of the fluence at the innermost tracking layer, their spectrum ranging between 1 MeV and 5 GeV. Preliminary results of a study [9] with reactor neutrons (~ 1 MeV) indicate damage a factor of 6 ± 1 larger than those of 24 GeV protons. The same diamonds measured in the CERN SPS test-beam exhibit about 50 % larger charge collection at the highest fluence than measured with the ^{90}Sr source in [9], indicating a relative factor of 4 for the neutron damage. These results match rather well the DPA prediction [8], while NIEL predicts only 40 % larger damage, albeit for both predictions the comparison was taken at the lowest given point at 10 MeV and not around 1 MeV. Using DPA scaling and averaging over the neutron spectrum, neutrons should contribute about 20 % to the total radiation damage or a quarter of that of pions. Thus the final prediction of charge from a pCVD ($CCD_0 = 200 \text{ } \mu\text{m}$) diamond detector after 10^{16} cm^{-2} of hadron fluence at HL-LHC is about 2000 e_0 , with large and hard to be estimated uncertainties mainly resulting from the non-established scaling of proton damage to pions, and scaling of neutron damage across the spectrum.

5. ATLAS Beam Monitoring

Currently diamond sensors have found application as beam monitoring devices in all LHC detectors. ATLAS and CMS use diamond detectors both in particle counting (ATLAS BCM; CMS BCMF) and current integration mode (ATLAS BLM; CMS BCM1, BCM2). Both experiments plan an upgrade with diamond tracking telescopes, ATLAS with the DBM project and CMS with the Pixel Luminosity Telescope (PLT) project. The CMS activities being covered in [10], in further discussion we focus on ATLAS.

ATLAS BCM is described in detail in [11]. In eight modules, 4 per side, pairs of back-to-back 1 cm x 1cm pCVD diamond sensors are deployed. Read-out by fast electronics enables superb timing resolution with TOF between two modules measured at better than 1 ns. Based on

TOF signature beam-background events can be clearly distinguished from collision products. Stability of response and insensitivity to pile-up also promoted BCM to the preferred luminosity monitor of ATLAS. In addition six pad pCVD diamond sensors per side are hooked up to the LHC machine BLM system, replacing the ionization chambers as the current source. Current is monitored at 40 μ s intervals, and the beams aborted if the threshold is exceeded in the same time bin in two out of six sensors on each side. The LHC beams were aborted twice in 2011 upon a clear signature of an “UFO” (dust speck) traversing the LHC beam near ATLAS.

The success of diamond-based detectors led ATLAS to plan the installation of a diamond based luminosity and beam spot monitor – DBM. This project is executed in the scope of the ATLAS Insertable B-Layer (IBL) project [12]. 24 pCVD sensors, ~ 2 cm x 2 cm in size, will be grouped by three in eight telescopes pointing to the interaction point from the forward direction ($r \sim 60$ mm, $z \sim \pm 900$ mm). Sensors will be patterned into 26880 pixels ($50 \mu\text{m} \times 250 \mu\text{m}$) and read out with the FE-I4 pixel read out chip. When installed during the LHC shutdown in 2013/14 it will constitute the largest diamond tracking detector ever deployed in HEP.

References

- [1] CERN/LHCC Reports 97-3, 98-20, 2000-011, 2000-015, 2001-002, 2002-010, 2003-063, 2005-003, 2006-010, 2007-002, 2008-005,
<https://indico.cern.ch/materialDisplay.py?contribId=8&sessionId=0&materialId=slides&confId=194183>.
- [2] S. Zhao, “*Characterization of the Electrical Properties of Polycrystalline Diamond Films*”, Ph.D. Dissertation, Ohio State University (1994).
- [3] Diamond Detectors Ltd, 16 Fleetsbridge Business Centre, Upton Road, Poole, Dorset, BH17 7AF, UK.
- [4] Element Six Ltd, Kings Ride Park, Ascot, Berkshire, SL5 8BP, UK.
- [5] II-VI INFRARED, 375 Saxonburg Blvd, Saxonburg, PA 16056, United States.
- [6] P. Miyagawa, private communication,
https://twiki.cern.ch/twiki/bin/viewauth/Atlas/RadiationBackgroundSimulations#IBL_studies.
- [7] W. de Boer, J. Bol, A. Furgeri, et al., “*Radiation hardness of diamond and silicon sensors compared*,” Phys. Status Solidi A204(2007)3004-3010.
- [8] Steffen Müller, “*The Beam Condition Monitor 2 and the Radiation Environment of the CMS Detector at the LHC*”, PhD Thesis, University of Karlsruhe, CERN-THESIS-2011-085.
- [9] M.Mikuž, V. Cindro, S. Cline et al., “*Study of Polycrystalline and Single Crystal Diamond Detectors Irradiated with Pions and Neutrons up to $3 \times 10^{15} \text{ cm}^{-2}$* ”, 2007 IEEE Nuclear Science Symposium Conference Record, N44-5.
- [10] N. Odell, “*Measurements of the luminosity and normalised beam-induced background using the CMS Fast Beam Condition Monitor*”, these proceedings.
- [11] V. Cindro, D. Dobos, I. Dolenc, et al., “*The ATLAS Beam Conditions Monitor*”, JINST 3(2008)02004.